

# Novel Mesoporous Silicates with Two-Dimensional Mesostructure Direction Using Rigid Bolaform Surfactants

Dongyuan Zhao,<sup>†,‡,||</sup> Qisheng Huo,<sup>†,‡,⊥</sup> Jianglin Feng,<sup>†,§,#</sup> Jiman Kim,<sup>†</sup>  
Yongjin Han,<sup>†</sup> and Galen D. Stucky<sup>\*,†,‡</sup>

Department of Chemistry, Materials Research Laboratory, and Center for Quantized Electronic Structures, University of California, Santa Barbara, California 93106

Received October 20, 1998. Revised Manuscript Received July 15, 1999

In this paper we describe how pore-structure modification can be achieved in a highly ordered fashion through the use of bolaform surfactants containing a rigid unit in the hydrophobic chain. The silicate mesophase, SBA-8, synthesized using bolaform surfactants at room temperature, is a two-dimensional (2-D) pore structure with a centered rectangular lattice (space group *cm̄m*,  $1 < a/b < \sqrt{3}$ ), which has no reported lyotropic liquid crystal analogue. SBA-8 is thermally stable in air, and the surfactant can be removed by calcination to yield a mesoporous material with a high surface area ( $>1000 \text{ m}^2/\text{g}$ ). The unit cell parameter of the silicate mesostructure can be varied by adding gemini surfactants or by changing reaction temperature; a 2-D silicate mesophase (*M̄a*,  $a/b > \sqrt{3}$ ) and high quality hexagonal MCM-41 (*p6mm*,  $a/b = \sqrt{3}$ ) can be obtained. Hydrothermal transformation of SBA-8 into MCM-41 takes place, confirming the intermediate nature of the SBA-8 mesophase.

## Introduction

The low-temperature formation of liquid crystal-like arrays made up of molecular assemblies of inorganic species and amphiphilic organic molecules is a convenient approach for the synthesis of mesostructured materials.<sup>1–12</sup> The pore and symmetry properties of these materials are largely determined by the organic

group structure and polarity. However, enhanced long-range order introduced by the use of charged surfactants along with kinetically controlled polymerization of the inorganic phase makes it possible to identify and characterize periodic structures not previously reported for conventional liquid crystal phases.<sup>11</sup> This is also evident for liquid crystal-like phases in general since the same relatively small collection of space-group symmetries are obtained for conventional amphiphilic and polymer systems even though the underlying compositions, molecular structures, and chemical and physical properties differ substantially.<sup>13–21</sup>

At the same time, it is becoming increasingly clear that the apparent limitation in the number of structural types is in reality a reflection of experimental difficulty in the characterization of less stable intermediate phases<sup>22</sup> and of shorter range order. The latter difficulty should be noted with respect to the comparatively small structural variations in modulated structures<sup>23</sup> that on the basis of conventional X-ray data are collectively

\* Author for correspondence. E-mail: stucky@chem.ucsb.edu.

<sup>†</sup> Department of Chemistry.

<sup>‡</sup> Materials Research Laboratory.

<sup>§</sup> Center for Quantized Electronic Structures.

<sup>||</sup> Present address: Professor Dongyuan Zhao, Department of Chemistry, Fudan University, Shanghai 200433, P. R. China.

<sup>⊥</sup> Present address: Dr. Qisheng Huo, Praxair, 175 East Park Drive, Tonawanda, NY 14151-0044.

<sup>#</sup> Present address: Dr. Jianglin Feng, Department of Molecular Physiology and Biophysics, University of Virginia, Charlottesville, VA 22908.

(1) Kresge, C. T.; Leonowicz, M. E.; Roth, W. J.; Vartuli, J. C.; Beck, J. S. *Nature* **1992**, *359*, 710. Beck, J. S.; Vartuli, J. C.; Roth, W. J.; Leonowicz, M. E.; Kresge, C. T.; Schmitt, K. T.; Chu, C. T.-W.; Olson, D. H.; Sheppard, E. W.; McCullen, S. B.; Higgins, J. B.; Schlenker, J. L. *J. Am. Chem. Soc.* **1992**, *114*, 10834.

(2) Zhao, D.; Feng, J.; Huo, Q.; Melosh, N.; Fredrickson, G. H.; Chmelka, B. F.; Stucky, G. D. *Science* **1998**, *279*, 548.

(3) Schacht, S.; Huo, Q.; Voigt-Martin, I. G.; Stucky, G. D.; Schüth, F. *Science* **1996**, *273*, 768.

(4) Huo, Q.; Margolese, D. I.; Ciesla, U.; Feng, P.; Gier, T. E.; Sieger, P.; Leon, R.; Petroff, P. M.; Schüth, F.; Stucky, G. D. *Nature* **1994**, *368*, 317.

(5) Huo, Q.; Margolese, D. I.; Ciesla, U.; Demuth, D. G.; Feng, P.; Gier, T. E.; Sieger, P.; Chmelka, B. F.; Schüth, F.; Stucky, G. D. *Chem. Mater.* **1994**, *6*, 1176.

(6) Tanev, P. T.; Pinnavaia, T. J. *Science* **1995**, *267*, 865.

(7) Monnier, A.; Schüth, F.; Huo, Q.; Kumar, D.; Margolese, D. I.; Maxwell, R. S.; Stucky, G. D.; Krishnamurty, M.; Petroff, P.; Firouzi, A.; Janicke, M.; Chmelka, B. F. *Science* **1993**, *261*, 1299.

(8) Stucky, G. D.; Monnier, A.; Schüth, F.; Huo, Q.; Margolese, D.; Kumar, D.; Krishnamurty, M.; Petroff, P.; Firouzi, A.; Janicke, M.; Chmelka, B. F. *Mol. Cryst. Liq. Cryst.* **1994**, *240*, 187.

(9) Zhao, D.; Huo, Q.; Feng, J.; Chmelka, B. F.; Stucky, G. D. *J. Am. Chem. Soc.* **1998**, *120*, 6024.

(10) Cheng, C. F.; Luan, Z.; Klinowski, J. *Langmuir* **1995**, *11*, 2815. Chen, C.; Li, H.; Davis, M. E. *Microporous Mater.* **1993**, *2*, 17.

(11) Huo, Q.; Leon, R.; Petroff, P. M.; Stucky, G. D. *Science* **1995**, *268*, 1324.

(12) Huo, Q.; Margolese, D. I.; Stucky, G. D. *Chem. Mater.* **1996**, *8*, 1147.

(13) Tiddy, G. J. T. *Phys. Rep.* **1980**, *57*, 1.

(14) Luzzati, V.; Vargas, R.; Mariani, P.; Gulik, A.; Delacroix, H. *J. Mol. Biol.* **1993**, *229*, 540.

(15) Henriksson, U.; Blackmore, E. S.; Tiddy, G. J. T.; Soderman, O. *J. Phys. Chem.* **1992**, *96*, 3894.

(16) Husson, F.; Mustacchi, H.; Luzzati, V. *Acta Crystallogr.* **1960**, *13*, 668.

(17) Hagslatt, H.; Soderman, O.; Jonsson, B. *Liquid Crystals* **1994**, *17*, 157.

(18) Jahns, E.; Finkelmann, H. *Colloid Polym. Sci.* **1987**, *265*, 304.

(19) Hagslatt, H.; Soderman, O.; Jonsson, B. *Langmuir* **1994**, *10*, 2177.

(20) Kratzat, K.; Finkelmann, H. *Colloid Polym. Sci.* **1994**, *272*, 400.

(21) Gulik, A.; Delacroix, H.; Kirschner, G.; Luzzati, V. *J. Phys. II* **1995**, *5*, 445.

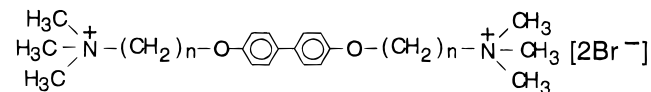
(22) Gallis, K. W.; Landry, C. C. *Chem. Mater.* **1997**, *9*, 2035.

assigned as isomorphous structures belonging to the collection of space-group symmetries noted above. Particularly for lyotropic mesophases of surfactants and lipids, it is very difficult to obtain clear conclusions about the exact nature of structures since the quality of the X-ray diffraction data is inadequate and high-quality electron microscopy data are difficult to obtain. In reality, the pore or cage shapes, wall thicknesses, and geometries of mesophases are highly tunable with almost an infinite variability. Inorganic mesophases with better long-range ordering and excellent stability are helpful in characterizing both new liquid crystal-like structures and structure modulations.

Within the range of liquid crystal phases<sup>13,15</sup> that can form in surfactant lyotropic systems, the name "intermediate phase" has been used for those noncubic phases occurring at compositions between hexagonal and lamellar phases.<sup>16,17</sup> Ribbon phases are the intermediate phases that appear closest to the normal hexagonal phase.<sup>17,24</sup> These phases are most easily described as a 2-D array of elongated noncircular tubes that are packed on 2-D lattices.<sup>25</sup> Experimentally, intermediate phases in charged surfactant systems are observed whenever the hydrophobic chain is rather long<sup>26,27</sup> and/or restricted in flexibility.<sup>28</sup> However, it is not clear why increasing the chain length or rigidity should favor the formation of these phases over the bicontinuous cubic structure.

Bolaform amphiphiles are closely related to gemini surfactants  $C_mH_{2m+1}N(CH_3)_2C_sH_{2s}N(CH_3)_2C_pH_{2p+1}Br_2$  (assigned  $C_{m-s-p}$ )<sup>11</sup> with two hydrophilic moieties connected by a hydrophobic chain (of length  $s$ ), but without the hydrophobic tails ( $m = p = 1$ ). Doubling the chain length seems to have a larger influence on the aggregation behavior than doubling the number of headgroups.<sup>29–31</sup> It has been predicted by theory and shown by experiments that surfactants containing rigid units have more specific aggregation behavior than conventional surfactants with a flexible hydrophobic chain.<sup>32</sup> In addition, introducing oxygen atoms into the bridging chain increases the solubility and makes it possible to substantially increase the bridging chain length. The unusual properties that result from these substitutions can be expected to introduce pore-channel size and shape anisotropy to the inorganic mesophase. For these reasons, the bolaform surfactants with rigid chain,

(designated as  $R_n$ ,  $n = 4, 6, 8, 10, 12$ ), were used as structure-directing agents in this study.<sup>33</sup>



## Experimental Section

**Chemicals.** Tetraethyl orthosilicate (TEOS) (Aldrich), NaOH (Aldrich), and 1,3,5-trimethylbenzene (TMB) (99%, ACROS) were used as received. Bolaform surfactants  $R_n$  ( $[(\text{CH}_3)_3\text{N}^+\text{C}_n\text{H}_{2n}\text{OC}_6\text{H}_4\text{C}_6\text{H}_4\text{OC}_n\text{H}_{2n}\text{N}^+(\text{CH}_3)_3]$   $[\text{2Br}^-]$ ,  $n = 4, 6, 8, 10, 12$ ) were prepared and purified as described in the literature.<sup>34</sup> Gemini surfactant  $C_{22-12-22}$  ( $C_{22}\text{H}_{45}\text{N}(\text{CH}_3)_2\text{C}_{12}\text{H}_{25}\text{N}(\text{CH}_3)_2\text{C}_{22}\text{H}_{45}$ ) was synthesized and purified as described previously.<sup>35</sup>

**Syntheses.** 1. *SBA-8 Mesophase.* A typical synthesis of SBA-8 is as follows. First, 0.6 g of bolaform surfactant  $R_{12}$  was mixed with 29 g of water and 3.6 g of (2 M) NaOH. To this solution was added 3.0 g of TEOS at room temperature, and the solution was stirred for 5 h or longer. The solid product was recovered by filtration on a Buchner funnel and dried in air at ambient temperature.

2. *Ma Mesophase.* A total of 0.25 g of  $R_{12}$  bolaform surfactant and 0.25 g of gemini surfactant  $C_{22-12-22}$  were dissolved in 35.6 g of water and 3.6 g of (2 M) NaOH. To this solution was added 3.0 g of TEOS at room temperature, and the solution was stirred for 24 h. The solid product was recovered by filtration on a Buchner funnel and dried in air at ambient temperature.

3. *MCM-41.* A total of 0.6 g of  $R_{12}$  bolaform surfactant and 0.6 g of TMB were mixed with 36 g of water and 3.6 g of (2 M) NaOH, and then 3.0 g of TEOS was added at room temperature and stirred for 5 h. The solution with solid was transferred into a Teflon bottle and heated at 100 °C for 3 days.

**Analyses.** X-ray powder diffraction patterns were taken on a Scintag PADX diffractometer using  $\text{Cu K}\alpha$  radiation. The nitrogen adsorption and desorption isotherms at 77 K were measured using a Micromeritics ASAP 2000 system. The data were analyzed by the BJH (Barrett–Joyner–Halenda) method using the Halsey equation for multilayer thickness. The pore-size distribution curve was calculated from the analysis of the adsorption branch of the isotherm. The pore volume was taken at  $P/P_0 = 0.985$  single point. Transmission electron micrographs (TEM) were taken on a 2000 JEOL electron microscope operating at 200 kV. The samples for TEM were prepared by dispersing a large number of particles of the products through a slurry in acetone onto a holey carbon film on a Cu grid.

## Results and Discussion

The powder X-ray diffraction (XRD) patterns of as-synthesized and calcined silicate mesostructure SBA-8 prepared using a bolaform surfactant with rigid chain, such as  $R_{12}$ , at room temperature, are shown in Figure 1. The XRD pattern of as-made SBA-8 shows two reflection peaks with  $d$  spacing of 41.3 and 37.9 Å, in the  $2\theta$  range of 2–2.5°, and several well-resolved diffraction peaks in the  $2\theta$  range of 3–10°. The XRD pattern can be indexed as a 2-D centered rectangular (space group *cm*) lattice with cell parameters  $a = 75.7$ ,  $b = 49.2$  Å,  $a/b = 1.53$  (Table 1). The bolaform surfactant in SBA-8 can be removed by calcination at high temperatures (500–600 °C). The XRD pattern of calcined SBA-8 at 500 °C in air shows that the (11) and (20) reflections shift to higher angles and some XRD peaks observed for as-made SBA-8 are too broad to be resolved. Four additional diffraction peaks are observed in the

(23) Firouzi, A.; Kumar, D.; Bull, L. M.; Besier, T.; Sieger, P.; Huo, Q.; Walker, S. A.; Zasadzinski, J. A.; Glinka, C.; Nicol, J.; Margolese, D.; Stucky, G. D.; Chmelka, B. F. *Science* **1995**, *267*, 1138.

(24) Hagslatt, H.; Soderman, O.; Jonsson, B. *Liq. Cryst.* **1992**, *12*, 667.

(25) With aqueous-rich *p6mm* liquid crystal phases, Vargas et al. have shown that the wall shape is hexagonal. As the surfactant/(surfactant + water) ratio is increased, the wall become more cylindrical. Vargas, R.; Mariani, O.; Gulik, A.; Luzzati, V. *J. Mol. Biol.* **1992**, *225*, 137.

(26) Burgoyne, J.; Holmes, M. C.; Tiddy, G. J. T. *J. Phys. Chem.* **1995**, *99*, 6054.

(27) Krämer, E.; Färster, S.; Göltner, C.; Antonietti, M. *Langmuir* **1998**, *14*, 2027.

(28) Kekicheff, P.; Tiddy, G. J. T. *J. Phys. Chem.* **1989**, *93*, 2520.

(29) Saupe, A. *J. Colloid Interface Sci.* **1977**, *58*, 549.

(30) Zana, R.; Yiv, S.; Kale, K. M. *J. Colloid Interface Sci.* **1986**, *77*, 456.

(31) Hessel, V.; Ringsdorf, H.; Laversanne, R.; Nallet, F. *Recl. Trav. Chim. Pays-Bas* **1993**, *112*, 339.

(32) Taylor, M. P.; Herzfeld, J. *Langmuir* **1990**, *6*, 911.

(33) A bolaform primary amine with a short flexible chain was previously used in the synthesis ( $\text{I}^{\text{S}}$ ) of a porous lamellar silica. Tanev, P. T.; Pinnavaia, T. J. *Science* **1996**, *271*, 1267.

(34) Kunitake, T.; Okahata, Y.; Shimomura, M.; Yasunami, S.; Takarabe, K. *J. Am. Chem. Soc.* **1981**, *103*, 5401.

(35) Zana, R.; Benrraou, M.; Rueff, R. *Langmuir* **1991**, *7*, 1072.

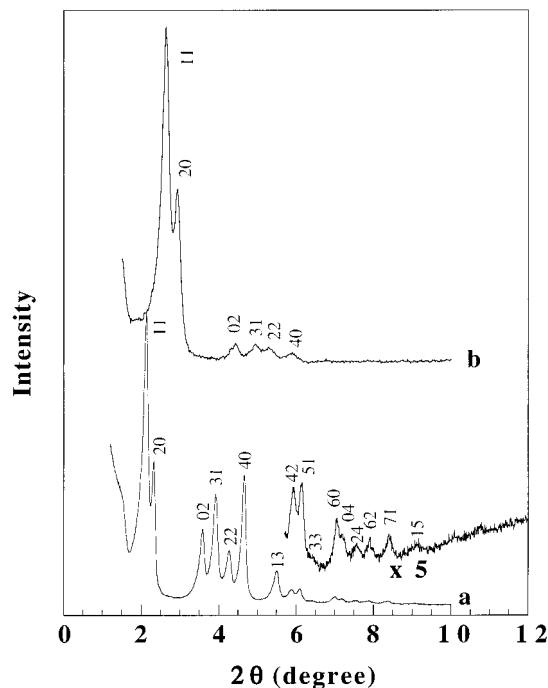


**Figure 1.** XRD patterns of (a) as-made SBA-8 and (b) calcined SBA-8.

**Table 1. Rectangular Cell Parameters for SBA-8, Silicate Mesophase  $M\alpha$ , MCM-41, and Relative Lyotropic Liquid Crystal Phase<sup>a</sup>**

mesophase	$a$ (Å)	$b$ (Å)	$a/b$
MCM-41 ( $p6mm$ )	79.2–80	45.7–46.4	$\sqrt{3}$
SBA-3 ( $p6mm$ )	77.6–77.9	44.8–45	$\sqrt{3}$
SBA-8 ( $cmm$ )	73.8–75.3	49.0–49.8	$\sim 1.5$
silicate $M\alpha$	91.1	44.2	2.06
SDS in water ( $p6mm$ )	76.8	44.3	$\sqrt{3}$
SDS in water ( $cmm$ )	87.4–101.8	39.6–37.2	2.2–2.8
SDS in water + NMF ( $p6mm$ )	74.4	43.0	$\sqrt{3}$
SDS in water + NMF ( $cmm$ )	83.2–90.8	38.6–36.7	2.1–2.5
CTAB in water ( $p6mm$ )	84.6	48.7	$\sqrt{3}$
CTAB in water ( $cmm$ )	95.2	43.4	2.2

<sup>a</sup> The  $p6$  hexagonal phase is indexed with rectangular symmetry,  $b = a_0$  (hexagonal cell) and  $a = \sqrt{3}a_0$ . MCM-41 samples are the result of a phase transition from SBA-8 at 100 °C in water. SBA-3 is synthesized using same surfactant  $R_{12}$  at room temperature in acid medium. The cells for SDS mesophases are after ref 37 and for CTAB from ref 42.

$2\theta$  range of 4–6.5 °, which can be indexed as (02), (31), (22), and (40) of centered rectangular  $cmm$  with cell parameters  $a = 60.0$ ,  $b = 39.6$  Å,  $a/b = 1.51$ . The relatively large cell contraction (20%) is due to uncompleted condensation of the siloxane framework resulting from low-temperature (room temperature) synthesis.

Transmission electron microscopy (TEM) images and electron diffraction patterns (Figure 2a,b) of calcined SBA-8 show a cylinder array along the [11] zone plane and a distorted hexagonal array along the [10] zone plane, confirming that calcined SBA-8 has a highly ordered 2-D mesostructure with centered rectangular symmetry. The cell parameters from TEM measurements are consistent with those from XRD measurements, indicating that SBA-8 is a thermally stable 2-D ( $cmm$ ) mesostructure.

The  $N_2$  adsorption–desorption isotherms of calcined SBA-8 prepared using  $R_{12}$  at room temperature are type-IV curves without hysteresis<sup>36</sup> (Figure 3), which is similar to that of small-pore MCM-41.<sup>37</sup> The analysis

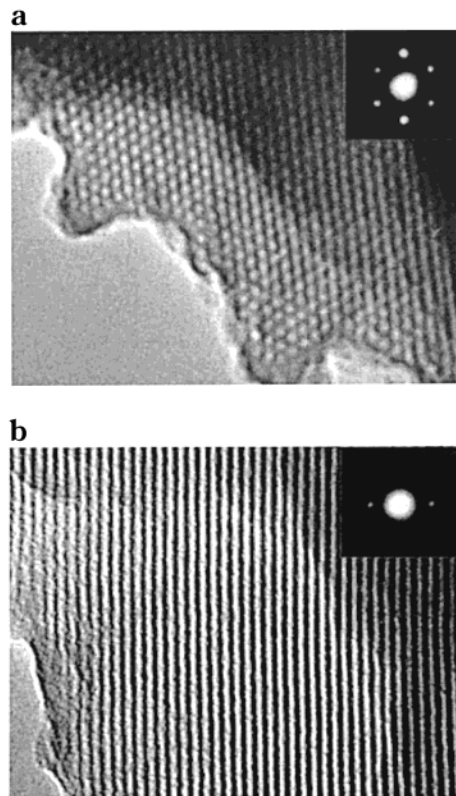


**Figure 2.** Lattice image and electron diffraction patterns (inset) of transmission electron micrographs for SBA-8 (a) perpendicular to channels and (b) parallel to channels.

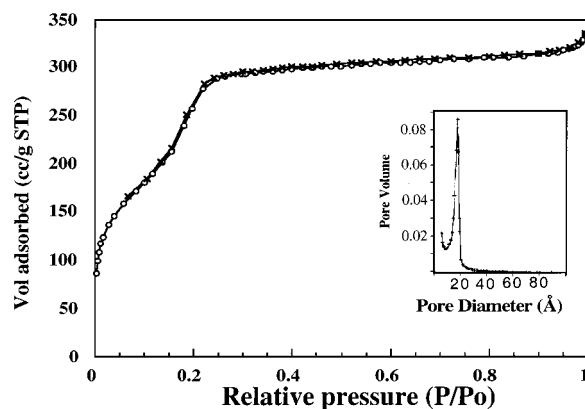


**Figure 3.** Nitrogen adsorption–desorption isotherm plots of calcined SBA-8. The inset is the corresponding pore-size distribution curve.

of surface areas of pores in this size range has been the subject of considerable discussion; however, the adsorption/desorption isotherm confirms excellent quality, high surface area pores.  $N_2$  BET analysis, which is qualitative at best, suggests a surface area of 1020  $m^2 g^{-1}$ .

The cell parameters of the silicate mesostructures can be varied by adding gemini surfactant or by changing reaction temperature. For example, 2-D silicate mesophase  $M\alpha$  ( $a/b > \sqrt{3}$ ) can be synthesized in the presence of gemini  $C_{22-12-22}$  and bolaform  $R_{12}$  surfactants at room temperature. The XRD pattern (Figure 4a) of this material shows two strong reflection peaks in the  $2\theta$  range of 1.5–2.5 °, with four additional peaks

(36) Sing, K. S. W.; et al. *Pure Appl. Chem.* **1985**, *57*, 603.

(37) Branton, P. J.; et al. *Faraday Trans.* **1994**, *90*, 2965.

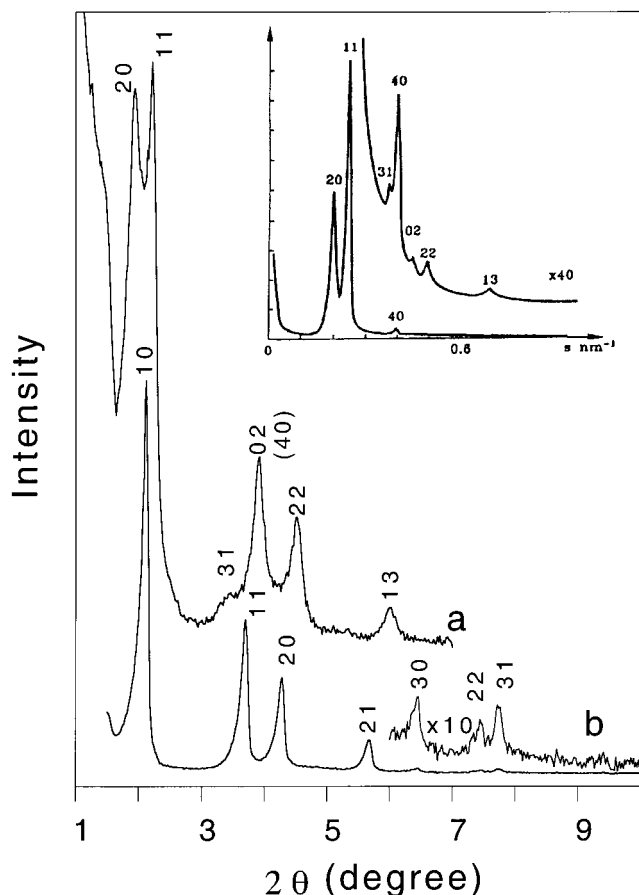


**Figure 4.** XRD patterns of (a) as-made silicate mesostructure  $M\alpha$  and (b) high-quality as-made MCM-41. Inset is XRD pattern obtained in SDS surfactant/water binary system from ref 31.

in the  $2\theta$  range of  $3\text{--}6^\circ$ . The well-resolved XRD pattern can be indexed as a 2-D centered rectangular ( $cmm$ ,  $M\alpha$ ) lattice with cell parameters  $a = 91.1$ ,  $b = 44.2$  Å,  $a/b = 2.06 > \sqrt{3}$ . This is in close agreement with that of the mesophase  $M\alpha$  formed in a sodium dodecylsulfate (SDS) surfactant/water binary system (Figure 4 inset).<sup>38</sup> On the other hand, high-quality 2-D hexagonal ( $p6mm$ ) mesostructure (MCM-41) can be synthesized using the same bolaform surfactant at high temperature ( $100^\circ\text{C}$ ). The XRD pattern (Figure 4b) of as-made MCM-41 shows seven well-resolved diffraction peaks with  $d(100)$  spacing of 41.8 Å.

In the SBA-8  $cmm$  structure ( $a/b < \sqrt{3}$ , Figure 5a), the elongation of the hexagonal channels (Figure 5b) takes place along the  $b$  direction and shrinkage takes place along the  $a$  direction (Figure 5a), while in the  $M\alpha$  structure the elongation is along the  $a$  direction and shrinkage is along the  $b$  direction (Figure 5c). A comparison of the cell parameters known for the  $cmm$  phases is given in Table 1. The relative intensities of the XRD reflections are similar to those<sup>39,40</sup> of the lyotropic mesophase  $M\alpha$  ( $a/b > \sqrt{3}$ ) of surfactant systems, e.g., SDS and cetyltrimethylammonium bro-

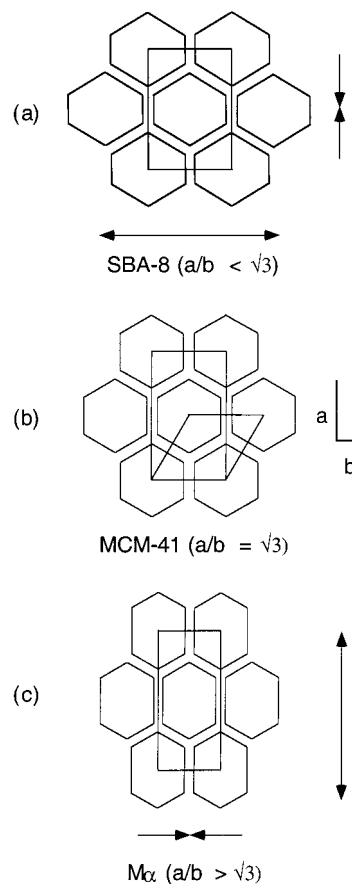


**Figure 5.** A scheme for deformation of 2-D hexagonal mesophase into 2-D centered rectangular mesophase.

mid (CTAB), although their relative positions ( $d$  values) do not match due to the different cell parameter  $a/b$  ratios. TEM studies of SBA-8 further support this result. There is, to the best of our knowledge, no reported evidence for the existence of a  $cmm$  lyotropic liquid crystal mesophase with  $a/b < \sqrt{3}$ , that is, of an analogue of SBA-8.

Transforming the normal 2-D hexagonal unit cell into the corresponding lower-symmetry centered rectangular cell (Figure 5) gives a unit cell ratio of  $a/b < \sqrt{3}$  or  $a/b > \sqrt{3}$ . Ribbon-phase  $cmm$  structures can be generated from the hexagonal  $p6mm$  phase by stretching out and contracting the hexagonal lattice along either the  $a$  or  $b$  direction of the rectangularly indexed unit cell of the hexagonal phase (Figures 5a and 5c). By convention  $a$  is chosen as the long direction of the resulting rectangular cell.<sup>17,24,41</sup> In the known examples of  $cmm$  structures of conventional liquid crystal phases, the deformation is as shown in Figure 5c, giving the  $M\alpha$  phase<sup>38,42</sup> with  $a/b > \sqrt{3}$ . These two symmetries are not readily distinguished due to the relatively small number of diffraction peaks observed in experiments with conventional lyotropic phases. Data for the  $M\alpha$  phase

(41) Hendriks, Y.; Charvolin, J. *J. Phys.* **1981**, *42*, 1427.

(42) The centered rectangular ( $cmm$ ) or monoclinic ( $p2$ ) symmetries have been proposed for the  $M\alpha$  phase. Rendall, K.; Tiddy, G. J. T.; Trevethan, M. A. *J. Chem. Soc., Faraday Trans. 1* **1983**, *79*, 637. Wood, R. M.; McDonald, M. P. *J. Chem. Soc., Faraday Trans. 1* **1985**, *81*, 273. Kekicheff, P.; Cabane, B. *J. Phys., Paris* **1987**, *48*, 1571.

(43) Auvray, X.; Petipas, C.; Anthore, R.; Rico, I.; Lattes, A. *J. Phys. Chem.* **1989**, *93*, 7458.

(44) Clerc, M. *J. Phys. II* **1996**, *6*, 961.

(38) Auvray, X.; Petipas, C.; Rico, I.; Lattes, A. *Liq. Cryst.* **1994**, *17*, 109.

(39) Auvray, X.; Petipas, C.; Anthore, R.; Rico-Lattes, I.; Lattes, A. *Langmuir* **1995**, *11*, 433.

(40) Auvray, X.; Perche, T.; Anthore, R.; Petipas, C.; Rico, I.; Lattes, A. *Langmuir* **1991**, *7*, 2385.

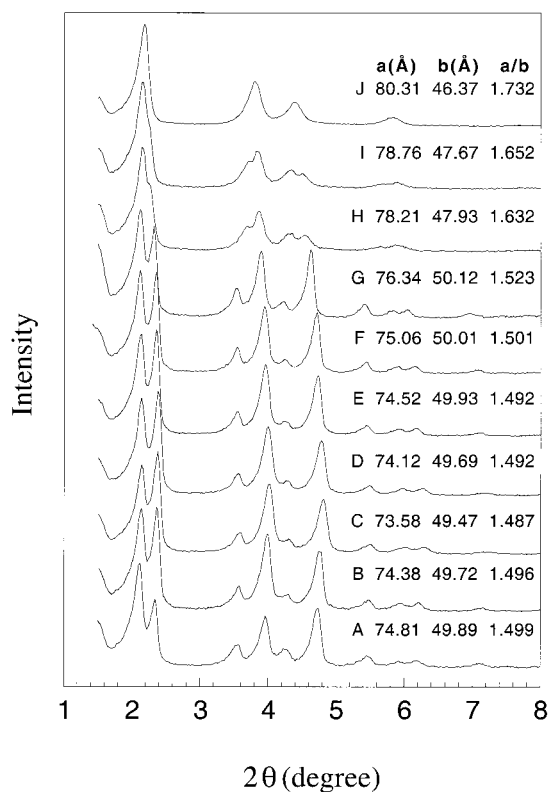


**Figure 6.** XRD patterns of observed mesophases in phase transitions (from SBA-8 to MCM-41): (A) SBA-8 obtained from a mixture with composition of 0.04 R<sub>12</sub>:0.5 NaOH:1 SiO<sub>2</sub>:150 H<sub>2</sub>O at room temperature for 8 h. (B–J) SBA-8 was treated hydrothermally: (B) at 70 °C for 8.5 h, (C) at 70 °C for 16 h, (D) at 70 °C for 29 h, (E) at 70 °C for 3 days, (F) at 70 °C for 15 days, (G) at 70 °C for 42 days, (H) at 70 °C for 16 h then at 100 °C for 6 h, (I) at 70 °C for 8.5 h and then at 100 °C for 6 h, and (J) at 100 °C for 15 h.

can be fitted with a centered rectangular lattice and there is no convincing experimental evidence to favor the existence of a monoclinic (*p2*) ribbon phase.<sup>17,24,43</sup>

Under basic synthesis conditions, the same type of surfactants R<sub>*n*</sub> (*n* = 10, 8, 6, 4) lead to the formation of MCM-41, and only the long-spacer surfactant R<sub>12</sub> yields SBA-8. This result is in agreement with the lyotropic behavior of long-rigid-chain surfactants.<sup>26,27</sup> On the

other hand, bolaform surfactants such as R<sub>12</sub> give SBA-3, the *p6mm* hexagonal phase, in acidic (HCl) solutions below the aqueous silica isoelectric point.<sup>4</sup>

A phase transition from SBA-8 to MCM-41 is found (Figure 6), confirming the intermediate nature of this phase. SBA-8 (*cmm*) can be induced to transform to MCM-41 (*p6mm*) in the mother synthesis solution or by treatment of as-made samples in water at 70–100 °C (pH = 7–10). Thus, SBA-8 synthesized at room temperature transforms readily into MCM-41 through postsynthesis treatment. When the as-made SBA-8 is treated in water at 100 °C, the phase transition to MCM-41 is completed within 2 h. The gradual transition can be controlled by varying treatment temperature and time. Existence of the intermediate product confirms that the transition occurs in the solid phase and not through dissolution to the liquid phase.

In summary, a novel silicate mesophase and transformation behavior of the silicate mesostructure has been found. The structure-directing role of rigid chain bolaform surfactants has been shown to result in excellent long-range order. SBA-8 is the second example of novel silica mesophases that we have found. The 3-D hexagonal silicate mesophase<sup>11</sup> SBA-2 has symmetry *P6<sub>3</sub>/mmc*, did not have a previously reported lyotropic liquid crystal structured analogue, and only subsequently was its lyotropic mesophase analogue found.<sup>44</sup> Inorganic mesophases with good long-range ordering and excellent stability are very helpful in the characterization of one of the less-studied intermediate symmetry phases and for further understanding of micelle and lyotropic liquid crystal phases of surfactant/molecular inorganic ion pairs. The discovery of SBA-2 and SBA-8 strongly suggests that other intermediate structured mesoporous phases with different wall structure and long-range symmetry synthesized by surfactant–inorganic self-assembly are accessible.

**Acknowledgment.** Funds were provided by NSF Grant DMR-95 20971 and by Air Products and Chemicals, Inc. This work made use of MRL Central Facilities supported by the National Science Foundation under Award No. DMR-9123048.

CM980755T